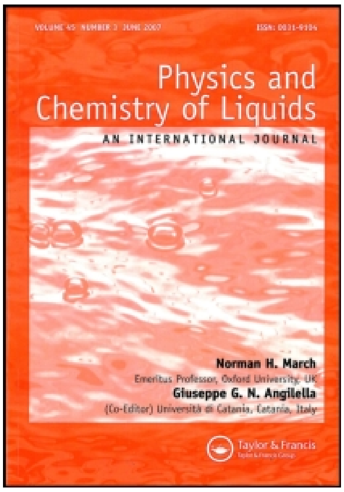

Physics and Chemistry of Liquids
Publication details, including instructions for authors and subscription information:
http://www.informaworld.com/smpp/title~content=t713646857

Separation of the Partial Structure Factors in Molten Copper Halides and Derivation of Dielectric Constants

Yoshiyuki Shirakawa[a]; Masatoshi Saito[b]; Yasutomo Arai[a]; Masanobu Kusakabe[c]; Shigeru Tamaki[d]
[a] Graduate School of Science and Technology, Niigata University, Niigata-ken, Japan [b] Institute for Advanced Materials Processing, Tohoku University, Miyagi-ken, Japan [c] Department of Applied Chemistry and Biotechnology, Faculty of Engineering, Niigata Institute of Technology, Niigata-ken, Japan [d] Department of Physics, Faculty of Science, Niigata University, Ikarashi, Niigata-shi, Niigata-ken, Japan

To cite this Article Shirakawa, Yoshiyuki , Saito, Masatoshi , Arai, Yasutomo , Kusakabe, Masanobu and Tamaki, Shigeru(1998) 'Separation of the Partial Structure Factors in Molten Copper Halides and Derivation of Dielectric Constants', Physics and Chemistry of Liquids, 36: 1, 1 — 16

To link to this Article: DOI: 10.1080/00319109808035916

URL: http://dx.doi.org/10.1080/00319109808035916

Phys. Chem. Liq., 1998, Vol. 36, pp. 1–16
Reprints available directly from the publisher
Photocopying permitted by license only

SEPARATION OF THE PARTIAL STRUCTURE FACTORS IN MOLTEN COPPER HALIDES AND DERIVATION OF DIELECTRIC CONSTANTS

YOSHIYUKI SHIRAKAWA[a], MASATOSHI SAITO[b], YASUTOMO ARAI[a], MASANOBU KUSAKABE[c] and SHIGERU TAMAKI[d]

[a]*Graduate School of Science and Technology, Niigata University, Ikarashi, Niigata-shi, Niigata-ken, 950-21 Japan;*
[b]*Institute for Advanced Materials Processing, Tohoku University, Katahira, Aoba-ku, Sendai-shi, Miyagi-ken, 980 Japan;*
[c]*Department of Applied Chemistry and Biotechnology, Faculty of Engineering, Niigata Institute of Technology, Fujihashi, Kashiwazaki, Niigata-ken, 945-11 Japan;*
[d]*Department of Physics, Faculty of Science, Niigata University, Ikarashi, Niigata-shi, Niigata-ken, 950-21 Japan*

(Received 30 July 1996)

The partial structure factors of molten copper haildes (CuCl,CuBr and CuI) have been derived from the observed total structure factors by means of the Reverse Monte Carlo simulation technique. The static dielectric functions are also obtained using these partial structure factors and it is found that these experimental dielectric functions satisfy either the inequality form $\varepsilon(q) \geq 1$ or $\varepsilon(q) < 0$.

Keywords: Reverse Monte Carlo; dielectric functions

1. INTRODUCTION

Some time ago, we have reported the total structure factors of molten copper halides by neutron diffraction measurements [1]. It was emphasized that the peak positions of the number–number density fluctuation S_{NN} and of the charge–charge density fluctuation S_{QQ}

denoted by q_N and q_Q, respectively, were within 0.56 to 0.60 which are much lower than those of molten alkali chlorides. By using the obtained total radial distribution functions and the Davidon-Fletcher-Powell [2] (hereafter referred to as DFP) method, an information for the partial configuration was also obtained. In particular, the peak position of Cu-Cu, Cu-Cl and Cl-Cl in molten CuCl are almost agreed with those obtained by the isotope-enrich method [3].

Another interesting fact for molten copper halides is that there has seen a prepeak in their structure factors which were modelized by a formation of the tetrahedral coordination due to the existence of a partially covalent bonding nature in them.

On the other hand, McGreevy *et al.* [4] have developed a new technique deriving the structural configuration of liquid and amorphous materials, based on a standard Monte Carlo simulation method with Markov chain sampling so as to fit the experimental structure factor, which gives three dimensional particle configuration. This method is called as Reverse Monte Carlo(RMC) simulation. These situations encourage us to separate the partial structure factors of molten copper halides.

Using the experimental data for structure factors, RMC simulation can reproduce a particle configuration without any interatomic or interionic potentials. Therefore RMC allows us to be useful for modelling the structures of non-crystalline materials and has many advantages in multicomponent systems as an experimental tool for analyzing the data.

In order to support a usefulness of RMC simulation, Pustai and Tóth [5] carried out the comparison of the two independent particle configurations derived from a standard Monte Carlo and a Reverse Monte Carlo method. The obtained results from these two simulation techniques closely agree to each other for the distribution functions of molten alkali halides.

Several attempts of RMC simulation have previously been applied to molten alkali halides [6], to glasses [7], and to aqueous solution [8].

In this paper, we apply this method to molten cuprous halides whose structural data were obtained before as mentioned above, and discuss the local configuration of these system.

2. METHOD OF CALCULATION

The RMC method for studying the structure of atomic or ionic liquid has been described in detail by McGreevy and Pusztai [4].

The algorithm for this method is essentially simple. The conventional procedure can be summarized as follows:

1. We start with an initial configuration arrayed N particle in a cubic box of length L. The total number of the particles is 4096 in the present simulation. L is determined by taking into account the experimental density [9].
2. Normal periodic boundary conditions are applied, and the pair distribution function $g_{\mathrm{cal}}(r)$ is calculated, where the maximum value of r is taken as $r_{\max} = 10\text{Å}$.
3. A new configuration is generated by a random motion of one particle. Then the new pair distribution function $g'_{\mathrm{cal}}(r)$ with the interval distance $\Delta r = 0.1\text{Å}$ is calculated.
4. These two pair distribution functions are compared with the experimental data $g_{\mathrm{exp}}(r)$. Each difference between the calculated values and experimental ones for the pair distribution function normalized by σ_{exp} is then written as

$$\chi^2 = \sum_{i=1}^{100} \{g_{\mathrm{exp}}(r_i) - g_{\mathrm{cal}}(r_i)\}^2 / \sigma^2_{\mathrm{exp}}(r_i) \qquad (1)$$

$$\chi'^2 = \sum_{i=1}^{100} \{g_{\mathrm{exp}}(r_i) - g'_{\mathrm{cal}}(r_i)\}^2 / \sigma^2_{\mathrm{exp}}(r_i) \qquad (2)$$

   where σ_{exp} is the experimental error [10], which are estimated as 3% for the averaged value over the entire range of the distance r.
5. If $\chi'^2 < \chi^2$, the new configuration $g'(r)$ is accepted. If $\chi'^2 > \chi^2$, it is accepted with a small probability $\exp[(\chi'^2 - \chi^2)/C]$ where C being a constant.
6. When the new configuration is accepted, it becomes as the starting procedure. Otherwise the old configuration is retained. Then we repeat the process from step 3.
7. This procedure is repeated until the $g_{\mathrm{cal}}(r)$ approaches to $g_{\mathrm{exp}}(r)$ as far as difference is negligibly small.

In a RMC simulation loop, it is favorable to compare the experimental results with the calculation ones for the $S(q)$ rather than the $g(r)$ [10]. To do so, however, it is necessary to obtain $S(q)_{\mathrm{cal}}$ by the Fourier transformation from $g_{\mathrm{cal}}(r)$. Therefore, the truncation effect is inevitable except for the case of simulation with a very large amount of particles. Hence, we adopt the method of the comparison for $g(r)$ in present work.

RMC simulation is not easy to obtain a plausible configuration for the materials starting from a random configuration if we ignore the condition being suitable for the systems. As a matter of fact, Pusztai and Tóth [5] checked the dependence of final particle configuration on the starting condition for various cases.

In this work, we have used our experimental data of neutron diffraction [1]. For convenience, the observed total $S(q)$'s are shown in Figure 1. Then to perform RMC simulation of molten cuprous halides, we have kept the several conditions. The first condition was a

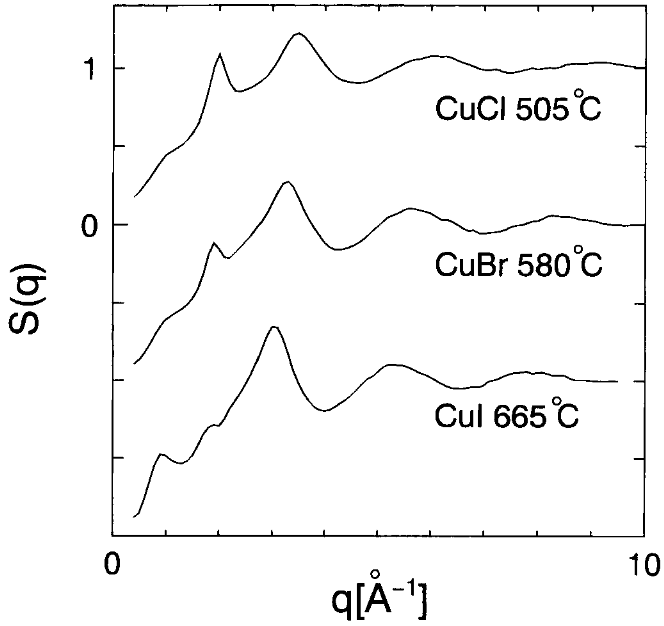

FIGURE 1 The observed total structure factor $S(q)$ [1].

restriction for the nearest neighbour distance d_{ii} between ions given by,

$$d_{\mathrm{CuX}} < d_{\mathrm{CuCu}} < d_{\mathrm{XX}} (\mathrm{X} = \mathrm{Cl}, \mathrm{Br}, \mathrm{I}).$$

The d_{CuX} is rather well determined by the sum of ionic radii of copper and halogen ions. However the distances of like ion pairs, d_{CuCu} and d_{XX}, were not well established. In concerning to this ambiguity, we have used the second condition that the ratio of the penetration of Cu ions to the first coordination shell is 25% or less otherwise a large amount of the first peak in $g(r)$ is governed by the Cu-Cu pair distribution [1]. Under these condition, RMC simulation has been performed, and we have obtained the results that the difference between the calculation $g_{\mathrm{cal}}(r)$ and the experimental $g_{\mathrm{exp}}(r)$ is quite small as shown in Figure 2.

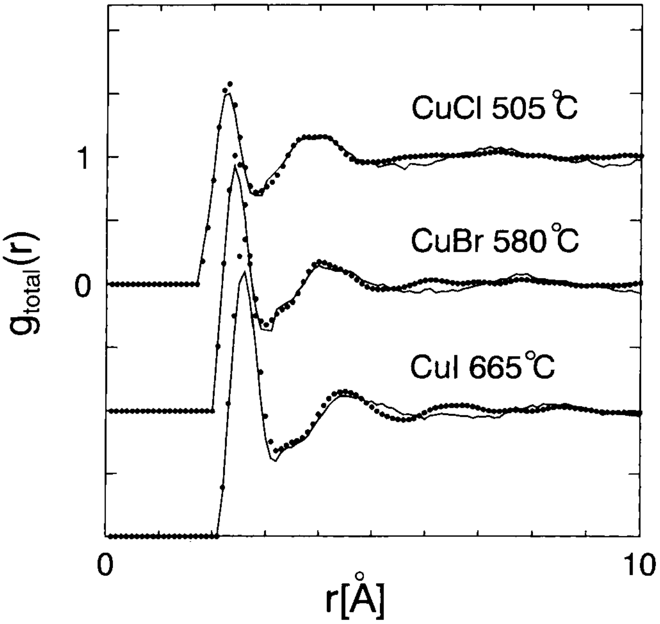

FIGURE 2 The total pair distribution function $g(r)$, solid line is the experimental $g_{\mathrm{exp}}(r)$ and dotted line is the calculated $g_{\mathrm{cal}}(r)$.

3. RESULTS

The partial pair distribution functions of molten CuCl in the Faber-Ziman type are shown in Figure 3. Results of molten CuCl in the present simulation agreed qualitatively and quantitatively well with those derived by the isotope enriched method [3] and by the theoretical calculation using HNC approximation [11] as shown in Figure 4. Cu-Cu distributions of RMC simulation for molten Cu halides also indicate a gas-like pattern. The correlations for unlike ion pairs molten CuBr and CuI are stronger than that of molten CuCl, because of more sharp first peaks in $g_{\mathrm{CuBr}}(r)$ and $g_{\mathrm{CuI}}(r)$. This behaviour is in accordance with those obtained by the isotope enriched method [12] and HNC calculation [11]. Another characteristic feature in Figure 3 is a broader distribution of the I-I pair in molten CuI.

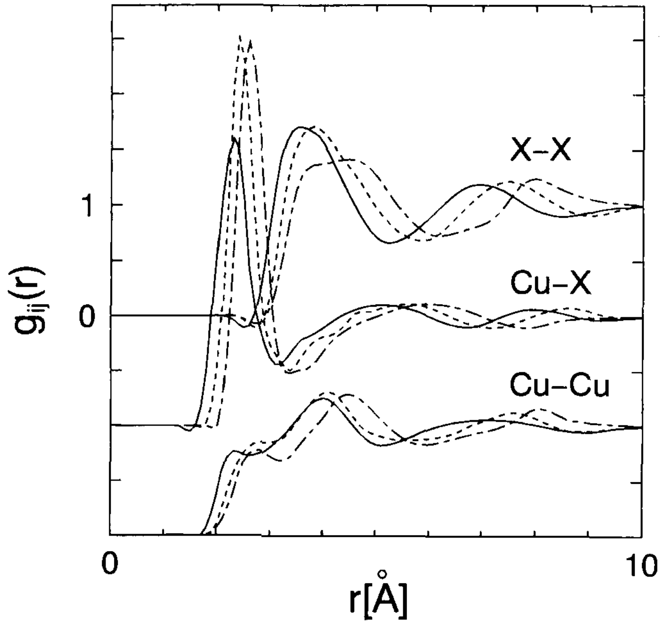

FIGURE 3 Partial structure factor $g_{ij}(r)$ at $T = 505°\mathrm{C}$ for molten CuCl, 580°C for molten CuBr and 665°C for molten CuI derived by means of RMC, solid line, molten CuCl, dotted line, molten CuBr, broken line, molten CuI, (X = Cl, Br, I).

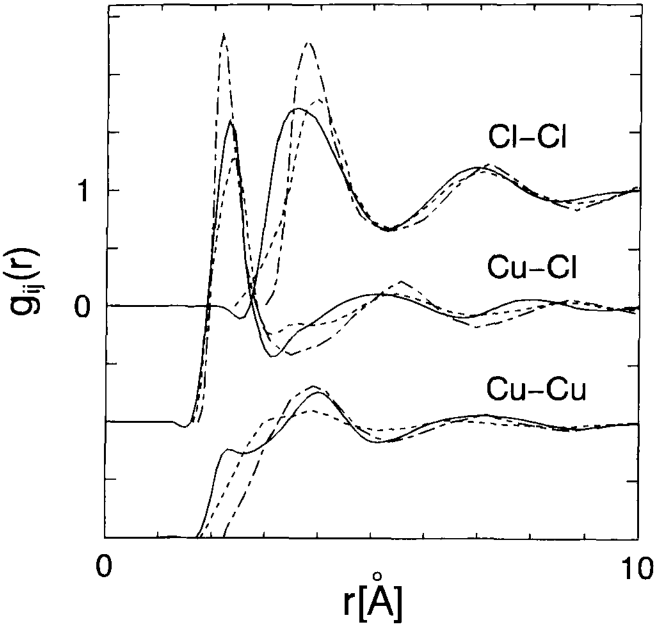

FIGURE 4 Partial structure factor of molten CuCl at $T = 505°C$, solid line; by RMC, dotted line; by isotope enriched method, broken line; by HNC approximation.

As is reported before, we have measured the total structure factors of molten copper halides and analyzed by using Davidon-Fletcher-Powell(DFP) method to extract some information on the partial structure factors [1]. The peak positions of Cu obtained by the present method agreed well with those by DFP one. All other peaks obtained by both methods are qualitatively and semiquantitatively agreed.

The bond angle distributions in Cu-X and X-X(X = Cl, Br, I) are shown in Figures 5 and 6. Their maximum angles in molten CuCl, CuBr and CuI are located at about 110° and 60° as seen in Figure 5 and Figure 6. These values indicate that molten CuCl, CuBr and CuI dominate a formation of the tetrahedral coordination. The peaks around about 110° due to the unlike ion pairs in molten CuBr and CuI are slightly sharper than that in molten CuCl. This corresponds to the results of the $g_{CuX}(r)$(X = Cl, Br and I).

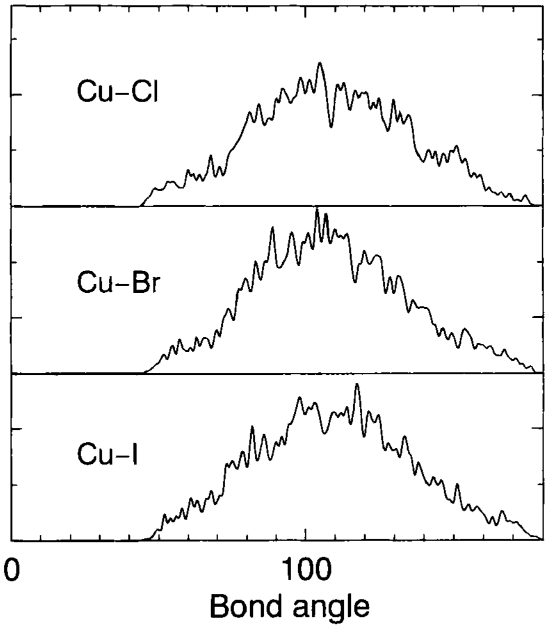

FIGURE 5 The bond angle distribution of unlike ion pair.

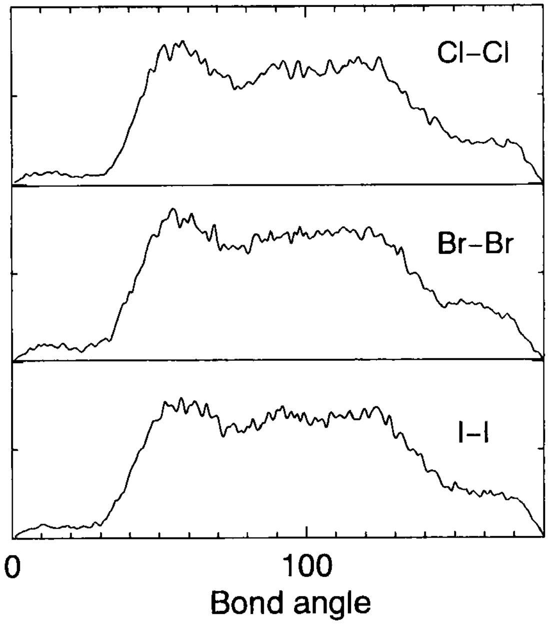

FIGURE 6 The bond angle distribution of anion pair.

In order to visualize the formation of tetrahedral coordination, some examples of RMC in the three dimensional configuration are shown in Figure 7.

As is shown in Figure 6, the bond angle distribution becomes less clear from Cl-Cl to I-I. On the other hand, the pre-peak at the low q region in the total structure factors $S_{\mathrm{total}}(q)$ of molten CuCl, CuBr and CuI increase by the order from CuCl to CuI [1]. These results may indicate that molten CuI behaves as molecular-like liquid, to some extent, and the intermolecule configuration may be more random compared to that of the intramolecule one.

By the Fourier transformation of the partial pair distribution function in molten copper halides, we have obtained the Ashcroft-Langreth type partial structure factors of molten CuCl, CuBr and CuI. In Figure 8, the curves of $g_{QQ}(r) = \frac{1}{2}[g_{++}(r) + g_{--}(r) - 2g_{+-}]$ are shown, which are the measure of the probability finding a charge of the same sign at a distance r from a given charge. If in the case that the effective charge of ions is equal to unity, then the Fourier transform of those curves gives the charge–charge correlation function which will be discussed in the following section.

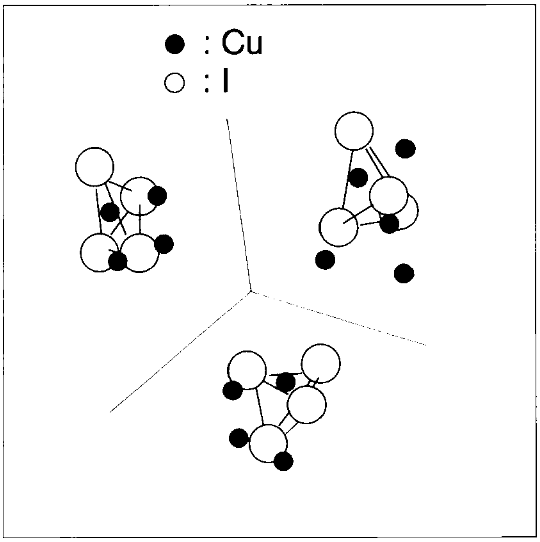

FIGURE 7 Examples of three dimensional configuration of tetrahedrons in molten CuI.

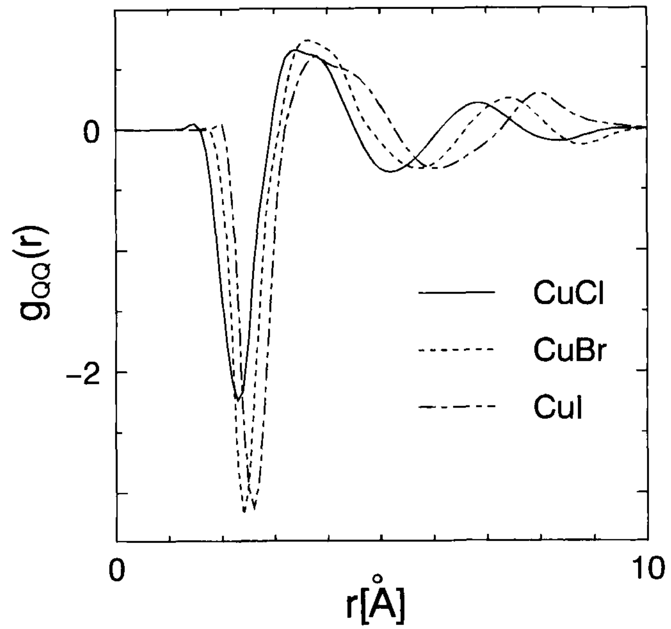

FIGURE 8 The distribution function $g_{QQ}(r)$ at $T = 505$°C for molten CuCl, 580°C for molten CuBr and 665°C for molten CuI.

4. STATIC DIELECTRIC FUNCTION OF MOLTEN Cu HALIDES

As mentioned in the preceding section, the results for molten CuCl are agreed with those obtained by the isotope enrich methods. These facts encourage us to discuss the microscopic response functions in relation to the partial structure factors.

The charge–charge correlation function $S_{QQ}(q)$ for a binary system is defined as follows[13],

$$S_{QQ}(q) = \sum_{\nu} \sum_{\mu} z_\nu z_\mu S_{\nu\mu}(q) \tag{3}$$

where z_ν is the effective charge of the ion constituent ν and $S_{\nu\mu}(q)$ is the Ashcroft-Langreth type partial structure between the constituents ν and μ.

Under the assumption that the electron-shell deformation is not taken into account, the static dielectric response function, χ_{QQ} and therefore the static dielectric screening function, $\varepsilon(q)$ are expressed as [13]

$$\chi_{QQ}(q) = \frac{-1}{k_B T}\rho_0 S_{QQ}(q) \tag{4}$$

and

$$\frac{1}{\varepsilon(q)} = 1 + \frac{4\pi e^2}{q^2}\chi_{QQ}(q) = 1 - \frac{\rho_0}{k_B T}S_{QQ}(q) \tag{5}$$

where ρ_0 is the averaged number density, k_B the Boltzmann constant and T the absolute temperature of the system.

By using the partial structure factors of molten CuCl, CuBr and CuI in the present investigation the charge–charge correlations S_{QQ}'s are obtained as shown in Figure 9. The small hump at an intermediate region between the first and the second peaks in these figures may be caused by the tetrahedral configurations in these molten salts, although a more definite relation is not clear.

Until the present time, it is often reported that the effective charges in these monovalent molten salts are not equal to the exact monovalent values because of the existence of some covalent bonding nature [14].

Taking into account this fact, we have tried to derive the two type of dielectric functions for $|z|=0.6$ and $|z|=1.0$. The obtained $\varepsilon(q)$'s are shown in Figures 10 and 11. These result are, of course, only valid for the strictly rigid ion model and we have to add some additional terms based on the electron-shell deforomation of the constituent ions for deriving exact dielectric functions.

As shown in Figure 12, $\varepsilon(q)$ for $|z|=0.6$ exhibits a fine structure, which becomes clearer in the order from molten CuCl to CuI. In the case of molten CuI, a distinct structure can be seen for only $|z|=0.6$ when $|z|$ varies from 0.5 to 1.

The obtained $\varepsilon(q)$'s have characteristic features as that $\varepsilon(q)$ has a negative value in the low q region as shown either in Figure 11 or Figure 12 and suddenly their values tend to be positive approaching to unity. At this point, the inverse dielectric energy loss becomes zero, that is, $Im\ \varepsilon(q,0)=0$, as will be discussed in the following section.

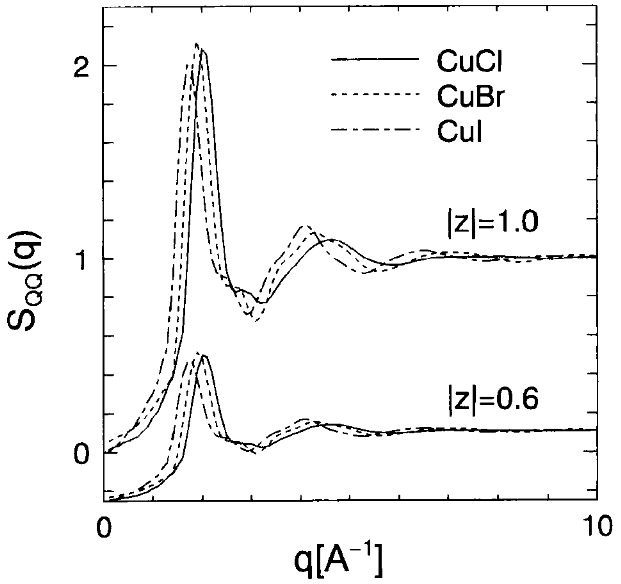

FIGURE 9 Structure factor $S_{QQ}(q)$ of effective charge $|z| = 0.6$ and $S_{QQ}(q)$ of $|z| = 1.0$ for molten Cu-halides.

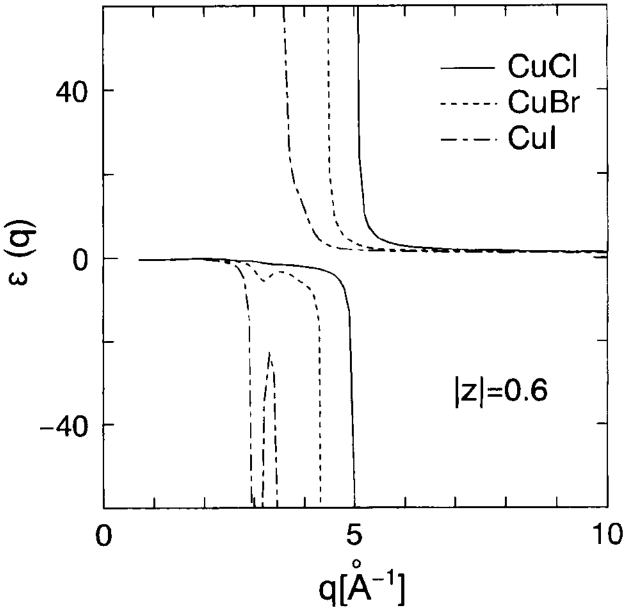

FIGURE 10 Static dielectric function of effective charge $|z| = 0.6$.

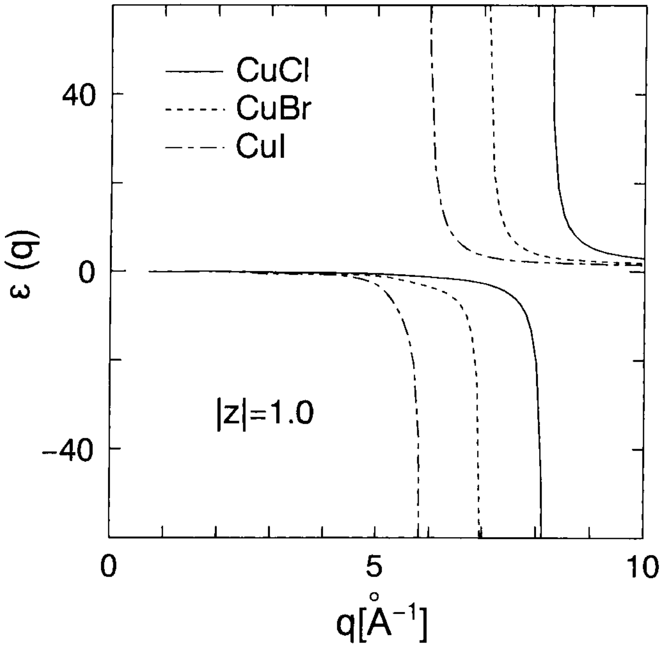

FIGURE 11 Static dielectric function of effective charge $|z| = 1.0$.

The curve of $\varepsilon(q)$ has a fine structure at around $q = 2\text{Å}^{-1}$ either in the case of $|z| = 0.6$ or in the case of $|z| = 1.0$. This fact may be related to the first peak of S_{QQ} because the first peak of S_{QQ} is located at around $q = 2\text{Å}^{-1}$. The behavior of $\varepsilon(q)$ at high q region is quite similar to the full screening by the conduction electrons for ions in metals. The drastic change of $\varepsilon(q)$ in the sign from negative to positive value may also resemble the dielectric function of conduction electric in metals, although it is hard to understand visually its singularity in the present scale range.

At the present stage, we can not determine which case either $|z| = 0.6$ or $|z| = 1.0$ is suitable for explaining the real situation because the present results are insufficient due to taking into account only the strictly rigid ions. However these treatments may be a step to develop the theory of molten salts.

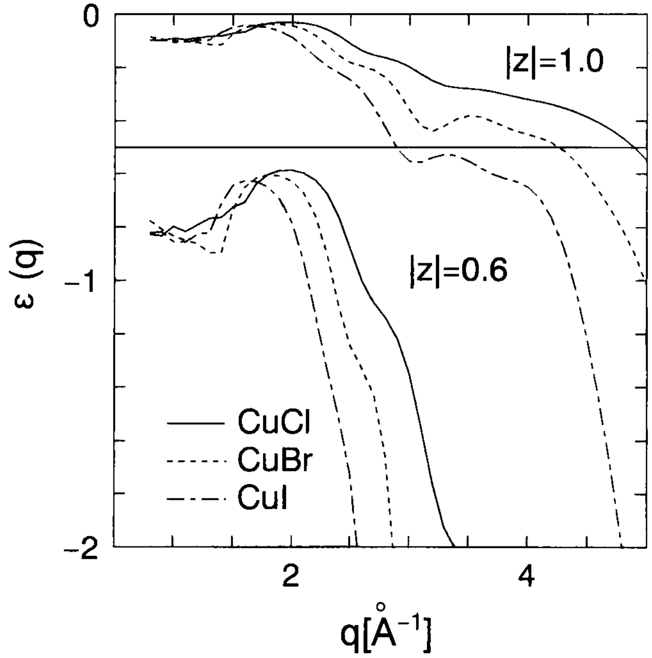

FIGURE 12 Static dielectric function $\varepsilon(q)$ of $|z| = 1.0$ and $\varepsilon(q)$ of $|z| = 1.6$ at a small q region.

5. DISCUSSION AND CONCLUSION

According to the causality condition expressed in terms of Kramers-Kronig relation, the inverse dielectric function $\varepsilon(q,\omega)^{-1}$ is given by the following form [13]

$$\varepsilon(q,\omega)^{-1} = 1 + \frac{1}{\pi}\int_0^\infty \frac{d\omega'^2 Im\varepsilon(q,\omega')^{-1}}{\omega'^2 - \omega^2 - i\delta} \tag{6}$$

In the static limit,

$$\varepsilon(q,0)^{-1} = \varepsilon(q)^{-1} = 1 + \frac{1}{\pi}\int_0^\infty \frac{d\omega'^2}{\omega'^2} Im\varepsilon(q,\omega')^{-1} \tag{7}$$

On the other hand, the inverse dielectric function is converted to the following form under the scheme of the fluctuation–dissipation theorem,

$$\frac{1}{\varepsilon(q,\omega)} = 1 + \frac{4\pi e^2}{q^2}\chi(q,\omega) \tag{8}$$

and

$$Im\frac{1}{\varepsilon(q,\omega)} = -\frac{\rho\omega}{2k_BT}\frac{4\pi e^2}{q^2}S(q,\omega) \tag{9}$$

where $\chi(q,\omega)$ is the density response function, ρ the number density and $S(q,\omega)$ the so-called dynamic structure factor. Taking into account $S(q,\omega) > 0$, we have

$$Im\varepsilon(q,\omega)^{-1} \leq 0 \tag{10}$$

Putting this into Equation (7), we finally obtain either

$$\varepsilon(q,0) \geq 1 \tag{11}$$

or

$$\varepsilon(q,0) < 0 \tag{12}$$

This is a general conclusion for the ionic static dielectric function and the present results satisfy these conditions. The values of momentum q_0 at the boarder either the dielectric function obeys Equation (11) or (12) may correspond to the points ending of the fine structure of $S_{QQ}(q)$, that is, the value of $S_{QQ}(q)$ becomes nearly flat for the higher momentum than the value q_0. As is shown in Figure 12, the fine structure in $\varepsilon(q)$ for molten Cu-halides can be seen around the value $q=2\text{Å}^{-1}$. This feature is quite similar to the cases of molten AgI and superionic phase of AgI [15].

From the present results, it can be seen that the Cu–Cu correlation becomes broader with changing the anion size from Cl^- to I^-, while the formation of tetrahedron is more appropriate on going from Cl^- to I^-. Therefore molten CuI may be composed of a distinct tetrahedron of four iodine ions surrounded by four copper ions disorderly.

These different behaviours between cation–cation and anion–anion correlation are caused by a large values for the ratio of anion size to cation one, and the gas-like correlation for cation–cation pairs is ascribed to an incomplete charge transfer which is recognized by molecular dynamics simulation study [16]. The configurations are determined by the ratio of ion size and the degree of charge transfer.

In conclusion, RMC simulation is very useful for analyzing X-ray and neutron diffraction data. But we pay attention of the initial condition of RMC, because ionic sizes noticeably determined can only reproduce plausible results.

References

[1] Shirakawa, Y., Saito, M., Tamaki, S., Inui, M. and Takeda, S. (1991). *J. Phys. Soc. Jpn.*, **60**, 2678.

[2] Fletcher R. and Powell, M. J. D. (1963). *The Computer Journal*, **6**, 163.

[3] Eisenberg, S., Jal, S. F., Dupuy J., Chieux P. and Knoll, W. (1982). *Phil. Mag.*, **A46**, 195.

[4] McGreevy R. L. and Pusztai, L. (1990). *Proc. Roy. Soc. Lond.*, **A430**, 241.

[5] Pusztai L. and Toth G. (1991). *J. Chem. Phys.*, **94**, 3042.

[6] Baranyai, A., Ruff, I. and McGreevy. R. L. (1986). *J. Phys.*, **C19**, 453.

[7] Keen D. A and McGreevy, R. L. (1990). *Nature*, **344**, 423.

[8] Howe, M. A. (1990). *J. Phys. Cond. Mat.*, **2**, 741.

[9] Inui, M., Takeda S. and Uechi, T. (1991). *J. Phys. Soc. Jpn.*, **9**, 3190.

[10] Kaplow, R., Strong S. L. and Averbach, B. L. (1965). *Phys. Rev.*, **138A**, 1336.

[11] Stafford, A. J., Silbert, M., Trullas J. and Giro A. (1990). *J. Phys. Cond. Mat.*, **2**, 6631.

[12] Allen D. A. and Howe, R. A. (1992). *J. Phys. Cond. Mat.*, **4**, 6029.

[13] March N. H. and Tosi, M. P. (1984). *Coulmb liquids* (UK London).

[14] Phillips, J. C. (1970). *Rev. Mod. Phys.*, **42**, 317.

[15] Aniya, M. (1991). *Ph. D. thesis in Niigata Univ.*

[16] Trullas, J., Giro, A., Padro J. A. and Silbert, M. (1991). *Physica*, **A171**, 384.